# Synthesis of Silver Nanoparticles Mediated by Cenchrus Biflorus for Lead(II) Sensing and Catalytic Reduction of 4-Nitrophenol

**Muhammad Bilal**
Kohat University of Science and Technology
**Majid Ali**
majidali58352@gmail.com

Kohat University of Science and Technology https://orcid.org/0009-0005-5082-4571
**Rehana Yasmeen**
Kohat University of Science and Technology
**Muhammad Qasim**
Kohat University of Science and Technology

**Research Article**

**Keywords:** Cenchrus Biflorus, Silver Nanoparticles, Green Synthesis, Reduction of 4-Nitrophenol

**Posted Date:** June 5th, 2025

**DOI:** https://doi.org/10.21203/rs.3.rs-6703901/v1

# SYNTHESIS OF SILVER NANOPARTICLES MEDIATED BY *CENCHRUS BIFLORUS* FOR LEAD(II) SENSING AND CATALYTIC REDUCTION OF 4-NITROPHENOL

**Muhammad Bilal[1] Majid Ali[*2] Rehana Yasmeen[*3] Muhammad Qasim[4]**

## Abstract

The present study provides a low-scale, cost-effective, and ecologically sustainable approach to producing silver nanoparticles using Cenchrus biflorus. Energy Dispersive X-ray analysis (EDX), Scanning Electron Microscope (SEM), Fourier Transform Infrared Spectroscopy (FTIR), UV-vis spectrophotometer, and X-ray Diffraction analysis (XRD) were employed to characterize the nanoparticles. Silver nanoparticles' optical properties were examined using a UV-VIS spectrophotometer, which showed an absorbance peak at 430 nm. through SEM analysis, the shape of silver nanoparticles was identified, and their sizes vary from 30 to 80 nm. FTIR analysis identified bioactive stabilizing agents present in the silver nanoparticles which included phenols along with flavonoids, triterpenoids, anthraquinones, amino acids, carbohydrates, and alkaloids. The researchers controlled the AgNPs reaction using the volumetric ratio (01 mL: 05 mL) along with pH (pH=8) and temperature (80 °C) and time (1 hour) and concentration (0.10 mM). Furthermore, the research describes AgNPs as a sensitive method for hazardous metal detection and organic dye removal. Research was conducted on the catalytic reduction of lead (II) and 4-nitrophenol. Under normal conditions, the Nano sensor probe demonstrated a sensitive response to $Pb^{+2}$ across a broad range of concentration (from 0.01 μM to 10 μM). 99.5% of 4-nitrophenol was broken down by AgNPs. Utilizing AgNPs for $Pb^{+2}$ detection and 4-nitrophenol catalytic reduction yields efficient, productive, and consistent outcomes.

**Key words:** Cenchrus Biflorus, Silver Nanoparticles, Green Synthesis, Reduction of 4-Nitrophenol

# 1.INTRODUCTION

Nanotechnology, also known as "nanoscience," is the study of the unique characteristics of materials with a diameter less than 100 nanometers (nm) in order to create new, profitable products. The capacity to change structures at the atomic level enables this study [1]. The development of incredibly small parts and systems is the focus of "nanotechnology," or "Engineering at the Molecular Level," an interdisciplinary field of applied science and engineering. They have a very large surface area relative to their volume, are created at the molecular level of matter, and behave in a way that is consistent with quantum physics [2].
Nanotechnology is based on nanoparticles with a one-dimensional size of less than 100 nm. Many fields of study, including the electrical, magnetic, optical, pharmaceutical, cosmetic, environmental, catalytic, and materials sciences, depend on nanoscale particles. As nanotechnology is an increasingly important subject and has applications in almost every scientific field, researchers from all over the world are interested in it [3]. These items are referred to as "nanoparticles" since their atomic diameters are $10^{-9}$ [4].

Metal nanoparticles (NPs) show a remarkable range of features when compared to bulk metal because they possess high surface-to-volume ratio along with low energy states density and nanometer-scale sizes [5]. Their strong chemical activity and selectivity make them more attractive for use as catalysts than bulk metals [6]. Due to their high surface-to-volume ratio and size effects, metal nanoparticles differ noticeably from bulk metal in terms of their chemical, electrical, optical, magnetic, and mechanical characteristics [7]. Nanoparticles demonstrated their utility in diverse applications including conductors, electronics, sensors, drug delivery, catalysis, fuel cells, light-emitting diodes, industrial lithographs, quantum devices and optical and biological devices during the previous two decades [8]. The special properties of nanoparticles are significantly affected by their tiny size, distinctive shape, surrounding medium, and production method. Thus, the production of metal nanoparticles is of interest of scientist [9].

Nowadays, there are various techniques for creating silver nanoparticles, including physical, chemical, and biological processes. Every method has advantages and disadvantages. To detect mercury in water, A. Adhikari and coworkers created silver nanoparticles (AgNPs) in 2022 using Artemis vulgaris. XRD showed the existence of crystal particles with an average size

of around 7 nm, and the UV/Vis spectra showed the formation of AgNPs with an SPR band at 418 nm. FTIR spectroscopy showed that the reducing agent of silver ions was an OH group which was part of the extract, whereas EDX confirmed the presence of silver. The sensitivity of the AgNPs to $Mg^{2+}$ was at 10 micromoles, while the color change was visible at 1 micromole, as well as the catalytic activity of the AgNPs in the reaction of 4-nitrophenol reduction. The rate constant for this reaction was $1.21 \times 10^{-2}$ $s^{-1}$ indicating the high activity of the AgNPs and their potential for green catalysis and metal sensing [10].

According to Doan et al. 2022, poria cocos extract was used to biosynthesize silver nanoparticles (AgNPs) in a green manner. The optimal conditions were 2.0 mM, 60 min reaction time, and 90 °C. XRD showed a crystalline face centered cubic structure, while TEM and FE-SEM showed spherical particles with an average size of 20 nm. FTIR, EDX and DLS results explain how biomolecules contribute to nanoparticle stabilization. The rate constant for the 4-nitrophenol reduction attained with PC-AgNPs was 0.466 $min^{-1}$ and it fully completed in ten minutes while carrying out five cycles exhibiting consistent results. Furthermore, they reported the detection of $Fe^{3+}$ ions with a high sensitivity of 1.5 μM as well as with high sensitivity and selectivity. The assay was tested on tap water with success, indicating the usage of PC-AgNPs as catalysts and biosensors for water monitoring [11].

An environmentally safe method for lignin-mediated synthesis of silver nanoparticles (L-AgNPs) using lignin biopolymers obtained through pulsed laser irradiation and ultrasonication has been described by Lee et al. 2021, as per the publication. Lignin itself functioned as reducing agent and stabilizing agent and produced non-aggregated spherical nanoparticles with 7–8 nm average size as confirmed by the structural analysis including TEM, UV-Vis spectroscopy and XRD. L-AgNPs sensitively detected hydrogen peroxide, and mercury ions through the comparison of antioxidant levels in water, and they chemically reduced noxious 4-nitrophenol and nitrobenzene to amino derivatives. Such environmentally-friendly Cu L-AgNPs well exemplify the potential of natural products, which gives a healthy way of reducing environmental pollution as well as biomedical applications [12].

Ahmed et al., 2020, reported green synthesis of silver nanoparticles (AgNPs) from Bistorta amplexicaulis root extract for sensitive, cost-effective colorimetric detection of $Hg^{2+}$ and $Pb^{2+}$.

Characterized via UV/Vis, FTIR, XRD, AFM, and Zetasizer, the AgNPs displayed visual SPR band changes upon metal interaction. Detection limits were $8.0 \times 10^{-7}$ M ($Hg^{2+}$) and $2.0 \times 10^{-7}$ M ($Pb^{2+}$). AgNPs also catalyzed methyl orange degradation, showcasing dual applications in sensing and catalysis [13].

Kaur et al., 2019, developed eco-friendly silver nanoparticles (AgNPs) from Psidium guajava leaf extract. The synthesis of AgNPs was confirmed through a 413 nm UV-Vis peak while the nanoparticles displayed monodispersity in the range of 20–30 nm. FTIR analysis revealed that the extract served as both a reducing agent and a capping agent. The AgNPs accelerated the 4-nitrophenol to 4-aminophenol conversion at a rate constant of 0.159 $min^{-1}$ through pseudo-first-order kinetics ($R^2 = 0.975$) during an 8-minute reaction time period [14].

Y. Shang et al., 2012 created a colorimetric Pb(II) detection system based on silver nanoparticles functionalized with iminodiacetic acid (IDA-AgNPs). A yellow to green color change occurred after Pb(II) exposure while the spectrum showed a new peak at 650 nm. The detection method exhibited linear behavior between Pb(II) concentration and absorbance ratio measurements (13 nM detection limit). It successfully detected Pb(II) in urea and tap water with recoveries of 93.7%–98.6% [15].

The study will focus on evaluating and treating diseases stemming from lead (II) and 4-nitrophenol exposure because these conditions prove fatal if medical attention is delayed. The detection of Pb (II) and the degradation of 4-nitrophenol occurred through the use of AgNPs. The study employs Cenchrus biflorus as a surfactant (capping agent) to enhance AgNPs characteristics while improving Pb (II) sensing and 4-nitrophenol catalytic reduction for better AgNP application outcomes.

## 2.METHODS AND MATERIALS

### 2.1 Preparation of extract

After carefully washing the leaves of the plants three times with deionized water to get rid of any dust, they were dried in the shade and crushed into a fine powder. Next, 5g of powdered cenchrus biflorus leaves were soaked in one hundred milliliters of distilled water and boiled on a hotplate for 30 minutes at 80 $^0$C the extract was filtered through Whatman paper before being

kept at 4°C for later usage. AgNPs were synthesized using this extract as a stabilizing and reducing agent.

.

**Figure.1** Cenchrus biflorus

**2.2 Synthesis of Silver nanoparticles**

Firstly, 0.0085g of $AgNO_3$ was added to 50mL of distilled water to create a 10 mM solution. Then, with constant, gentle stirring, 20 mL of the resulting extract solution was added drop by drop to the 50 mL of AgNO3 solution. Silver nanoparticles (AgNPs) begin to form when the solution's colour gradually shifts from yellow to a dark reddish brown. After that, centrifugation was done for one hour at 10,000 rpm. After that, ethanol and distilled water were used three times to clean the centrifuge. After that, the solid was removed and milled into a powder for further investigation [16].

**Figure 2.** Formation of AgNPs

### 2.3 Optimization and Characterization of Silver Nano particles

The synthesis of silver nanoparticles (AgNPs) was optimized by several parameters, including concentrations of silver nitrate ($AgNO_3$), volumetric ratios of $AgNO_3$ to extract, reaction time, pH, and temperature. Different concentrations of $AgNO_3$ (ranging from 10 mM down to 0.01 mM) were prepared using a dilution formula, and the volumetric ratios ranged from 1:1 to 40:1. Subsequently, nanoparticle formation was confirmed by using UV-Vis spectroscopy. The reaction time was optimized by stirring the mixture at intervals from 0 to 4 hours, and the pH effect was examined across values from 2 to 10. Temperature optimization involved shaking the reaction mixture at various temperatures from room temperature to 90°C. The synthesized AgNPs were characterized by using UV-Vis spectroscopy for optical properties, FTIR for functional group analysis, SEM for surface morphology, EDX for elemental composition, and XRD for crystallinity determination.

## 3. RESULT AND DISCUSSION

### 3.1 UV/Vis spectra of plant extract

Figure.3 shows the UV-Vis absorption spectrum of the plant extract in the range of 200–800 nm. In this spectrum, a prominent peak at 230 nm with a high absorbance value can be seen. This suggests that conjugated π-electron systems like aromatic compounds or other chromophores are present in the extract. Beyond 230 nm, the absorbance gradually decreased, and no significant peaks were observed in the visible region, suggesting that the extract primarily contains compounds that absorb in the UV region.

The sharp peak at 230 nm aligns with the electronic transitions typically associated with $\pi \rightarrow \pi^*$ transitions, which are characteristic of phenolic compounds, flavonoids, or other plant metabolites.

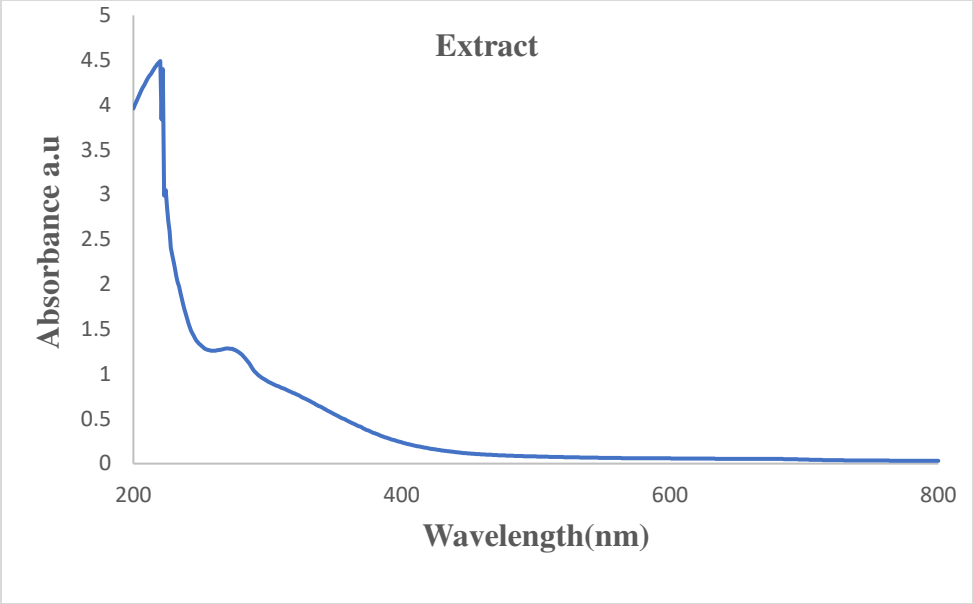


**Figure 3.** UV/Vis spectra of plant extract

### 3.2 Optimization of silver nitrate concentration

Different results are obtained by varying the concentration of silver nitrate. Various concentrations of $AgNO_3$ were combined with 1mL of extract to determine the ideal concentration. In order to determine absorbance, UV/Vis spectroscopy was used. Figure 4 indicates that the most effective concentration for producing high-quality silver nanoparticles is 0.1mM $AgNO_3$, as it was discovered to produce the best SRB band, which was intense and clean.

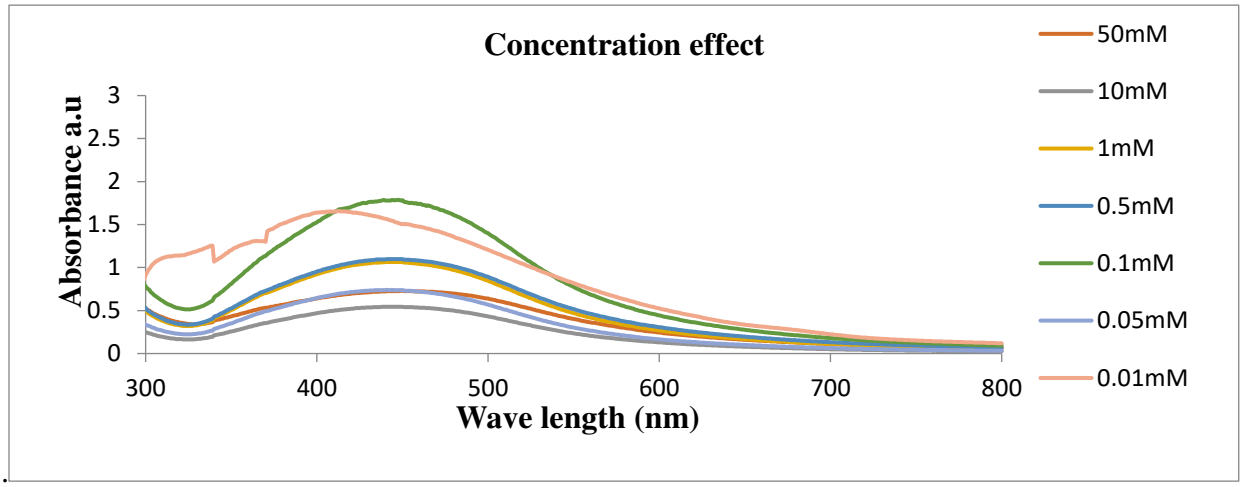

**Figure 4.** Uv/Vis spectra of AgNPs at different precursor concentrations

### 3.3 Volumetric ratio effect

Figure 5 presents AgNO3: Extract volumetric ratios in mL that range from 1:1 to 1:3 to 01:05 to 1:10 and 5:1 to 40:01 while 5 mL: 1 mL achieved the most effective result due to its sharp intense band.

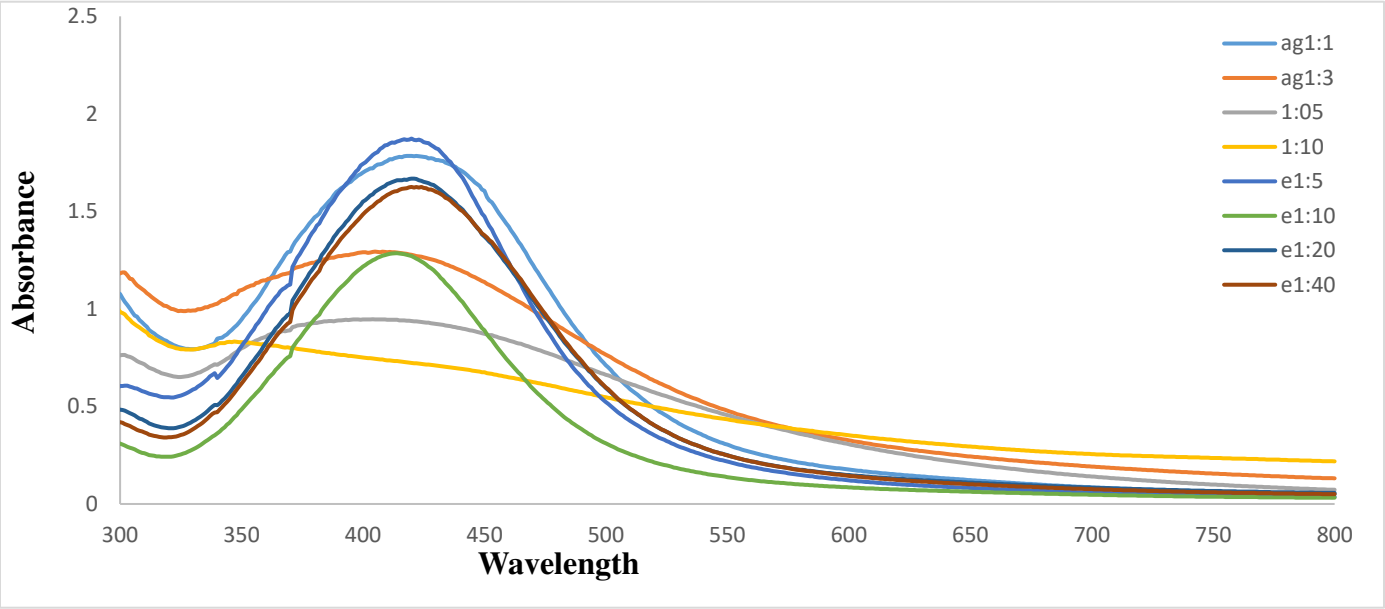


**Figure 5.** UV/Vis spectra at different volumetric ratio of AgNO3: Extract solutions

### 3.4 Reaction time optimization

A series of UV-visible spectra obtained at different reaction times showed the data collected in Figure 6. A peak wavelength situated at 423 nm appears in the absorption spectra of silver nanoparticles. The reaction produces reductions in metal ions throughout the 30 minutes' duration without distorting the peak wavelength while the intensity steadily increases during this process.

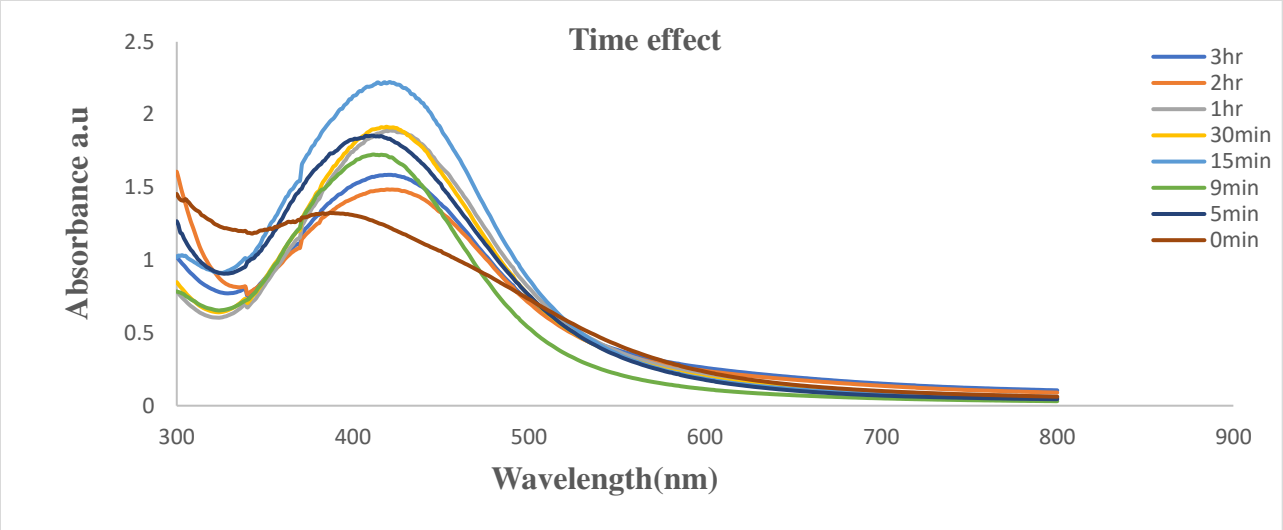


**Figure 6**. Reaction of nanoparticles at different time interval

### 3.5 Effect of pH

The investigated reaction solution initially displayed a pH reading of 8.. The pH was adjusted to the range of 2–10 using 0.1 M NaOH or HCl, and the synthesis of silver nanoparticles (AgNPs) was monitored by UV-Vis spectroscopy. As shown in Figure 7, the SPR absorbance band of AgNPs (400–450 nm) reached maximum intensity at pH 7, indicating optimal nanoparticle formation and stability. In contrast, there were no SPR peaks under acidic conditions, pH 2–5; this could be due to an incomplete reduction of silver ions or nanoparticles' aggregation due to protonation of stabilizing agents.

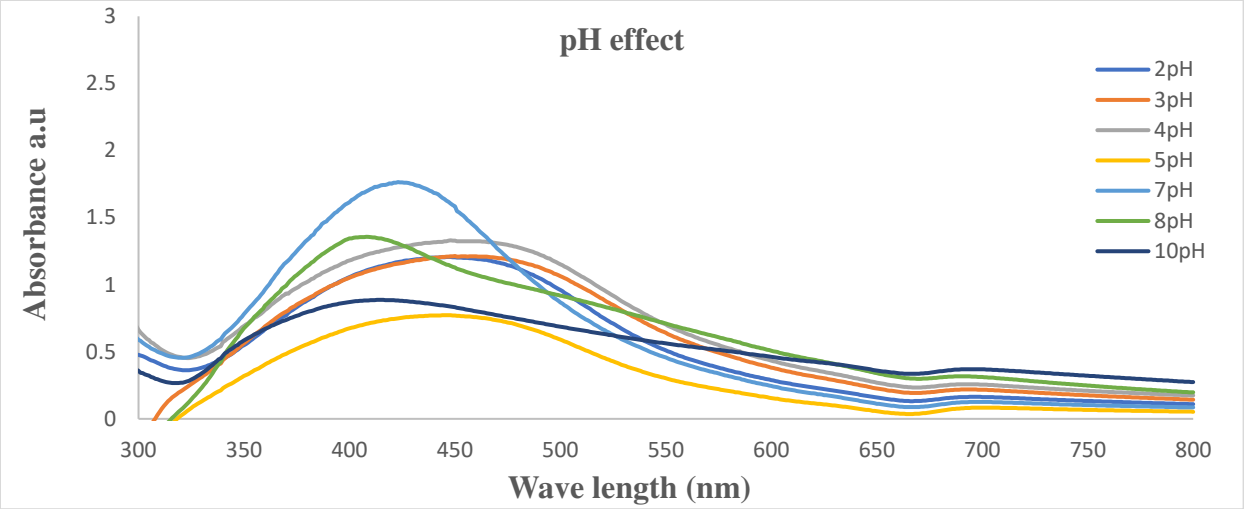


**Figure7.** UV/Vis spectra of AgNPs at different pH

### 3.6 Reaction temperature effect

The mixture of $AgNO_3$ and plant extract received tests at temperatures between 25 to 90 °C to study its effect on the synthesis of silver nanoparticles UV-Vis spectroscopy showed a sharp SPR band at 400–450 nm at 80°C, indicating the formation of monodisperse AgNPs with optimal size and stability as shown in Figure 8. At lower temperatures (25–70°C), weaker or broader SPR bands suggested slower reaction kinetics or polydispersity, while temperatures above 80°C resulted in reduced absorbance, likely due to thermal degradation of bioactive compounds in the extract or nanoparticle aggregation.

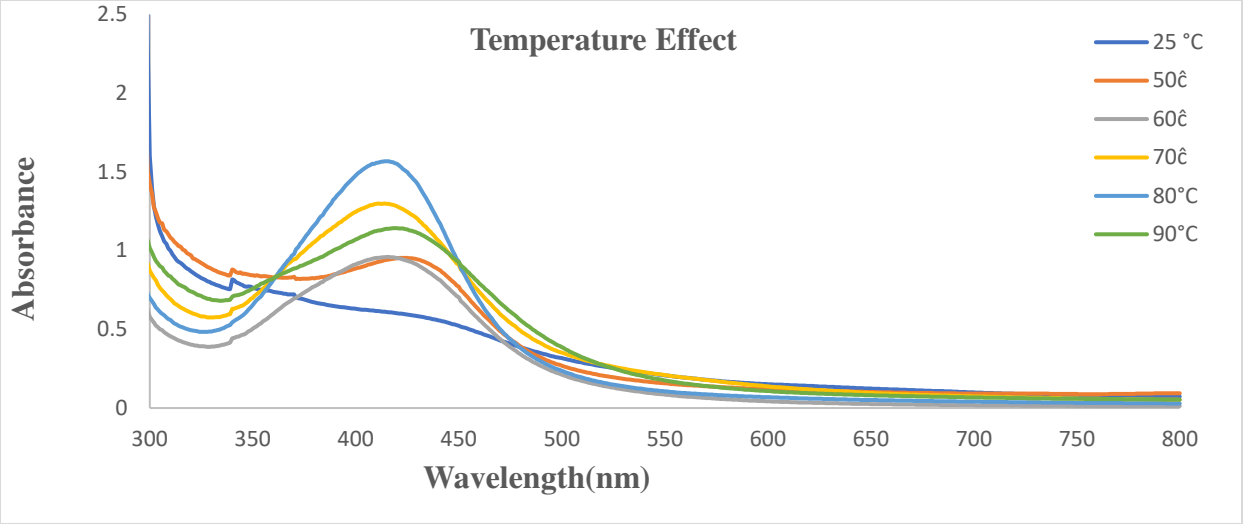


**Figure 8.** UV/Vis spectra of AgNPs at different temperature

### 3.7 UV/Vis spectroscopy of AgNPs

Results from UV-Vis spectroscopy helped to verify the formation of Silver nanoparticles, which presented a characteristic surface Plasmon resonance (SPR) band centered at 423 nm Figure 9. This peak in the absorption spectrum is associated with collective oscillation of the conduction electrons in AgNPs upon interaction with visible light, confirming the formation of spherical nanoparticles with diameters typically less than 50 nm. This suggests the presence of a monodisperse size distribution and therefore of controlled nucleation and growth in synthesis; narrow full-width-at-half-maximum (FWHM) of the SPR band.

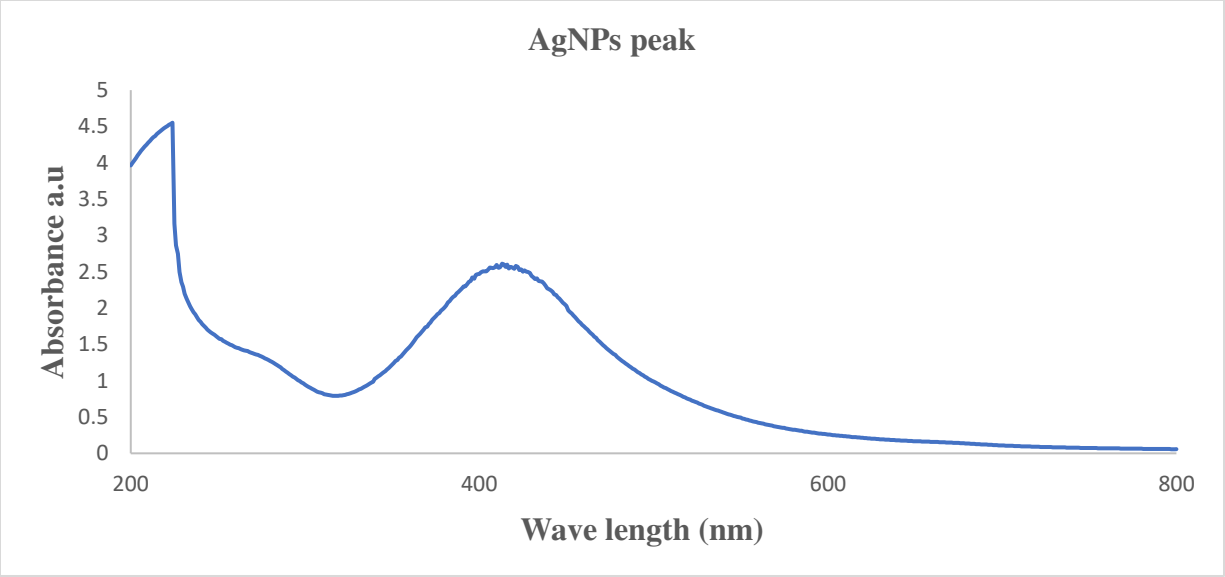


**Figure 9.** UV/Vis spectra of AgNPs

### 3.8 FTIR Analysis

FTIR analysis was performed to identify the functional groups of biomolecules present in the leaf extract of Cenchrus biflorus responsible for the reduction of silver ions to silver nanoparticles. The FT-IR spectra of the leaf extract (Fig. 10.A) and the green-synthesized silver nanoparticles (Fig. 10.B) were compared. Peaks at 1622cm$^{-1}$, 1480 cm$^{-1}$, and 1191cm$^{-1}$ are characteristic of flavanones and terpenoids, which are abundant in the leaf extract. The peaks at 1622 cm$^{-1}$ and 1480 cm$^{-1}$ indicate the presence of ether linkages and C=O groups, respectively. The peak at 1191 cm$^{-1}$ suggests the involvement of reducing compounds that facilitate the conversion of silver ions to silver nanoparticles. Terpenoids are thought to act as stabilizing agents, coating the surfaces of the nanoparticles, and their presence along with reducing sugars in the leaf broth enhances the reduction process.

The FT-IR spectra of the silver nanoparticles (Ag-NPs) have shown significant shifts compared to the leaf extract, which indicates the capping effect of the plant biomolecules on the nanoparticles. The spectra for Ag-NPs feature a distinct band located at 3317 cm$^{-1}$ which represents stretching motions of -OH groups. Symmetrical stretching vibrations of -CH groups were observed at 2933 cm$^{-1}$. At the same time, the stretching frequency of C=O shifted from 1622 cm$^{-1}$ in the extract to 1600 cm$^{-1}$ in the Ag-NPs. These spectral changes confirm that the -

OH and C=O groups in the biomolecules present in the leaf extract play a vital role in the stability of the nanoparticles. Practical applications are highly dependent on the stability of these Ag-NPs incorporated with Cenchrus biflorus against different conditions of pH, temperature, and electrolyte concentration [17].

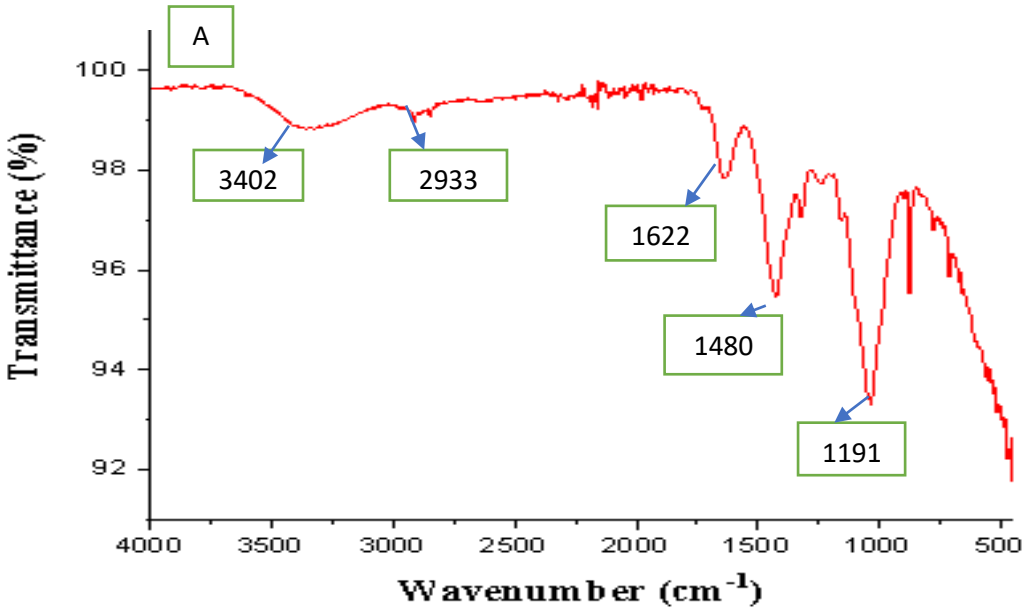


**Figure 10 A:** FTIR of Extract

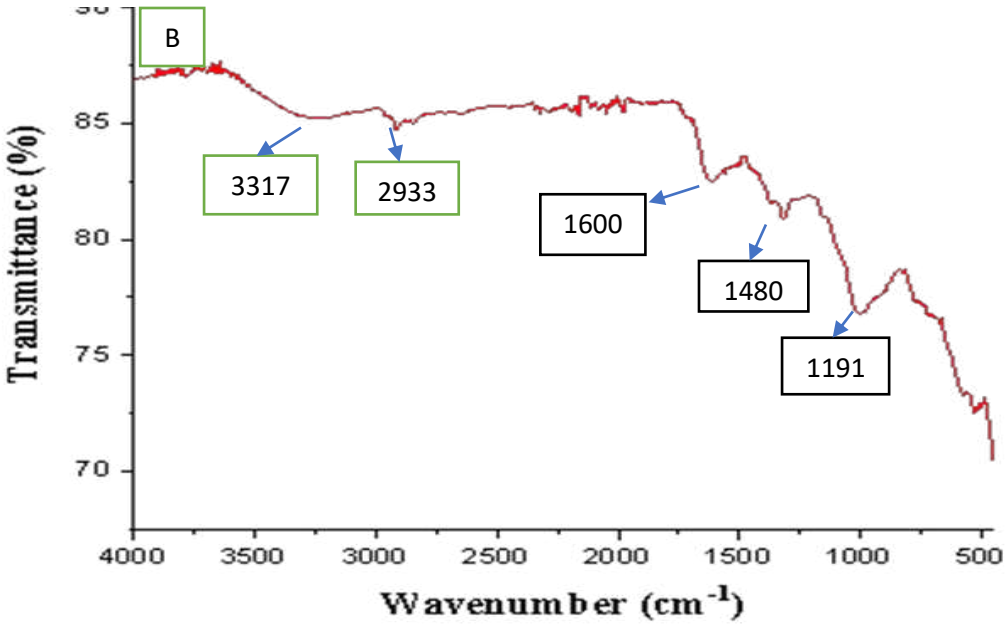


**Figure 10 B:** FTIR spectra of AgNPs

### 3.9 SEM Micrographs of Silver nanoparticles

The SEM system provides visual evaluation of nanoparticle dimensions alongside surface form and structural makeup. SEM images prominently revealed that there were nanoparticles. The shape of the nanoparticles was spherical. Because of the agglomeration of the nanoparticles, there were hardly any isolated particles. The size was predominantly uniform and was between 5 and 15 nanometers. Metal nanoparticles used in sensor experiments are typically spherical. These silver nanoparticles were again used to sense metal ions [18].

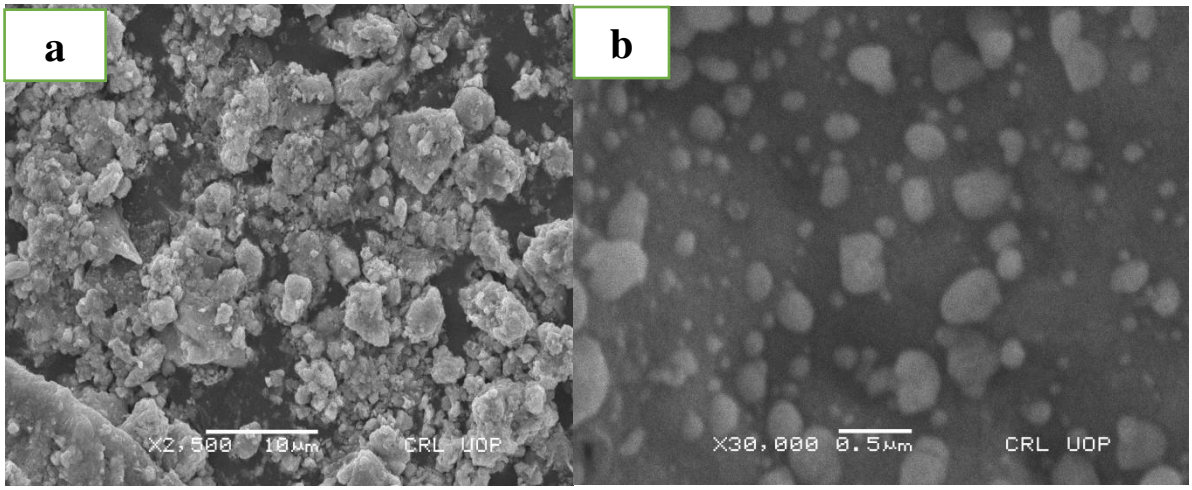


**Figure 11.** SEM images of AgNPs

### 3.10 EDX analysis

The energy dispersive X-ray analysis provides both quantitative and qualitative assessments of ingredients that may participate in the synthesis of AgNPs. The EDX analysis indicated that nanoparticles contained 77.56% weight of silver nanoparticles while atoms represented 34.27% of the sample as shown in Figure 12. [19].

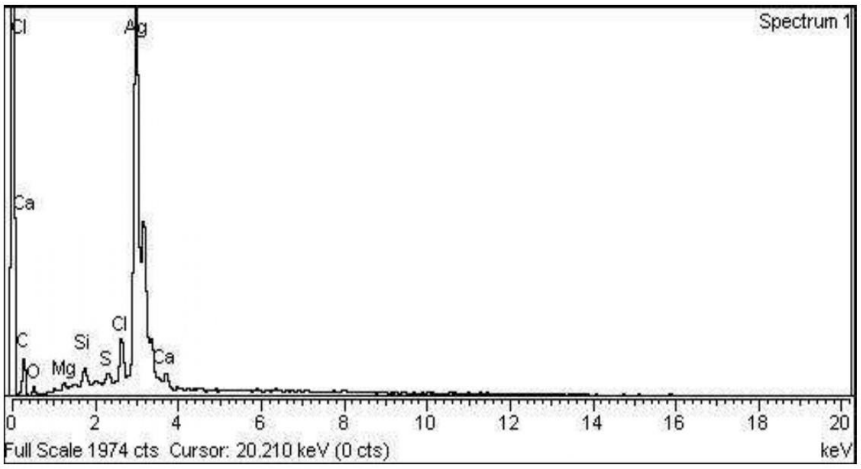


| Element | Weight% | Atomic % |
|---|---|---|
| C | 8.95 | 35.50 |
| O | 6.97 | 20.75 |
| Mg | 0.74 | 1.45 |
| Si | 1.19 | 2.01 |
| S | 0.73 | 1.09 |
| Cl | 2.12 | 2.86 |
| Ca | 1.74 | 2.07 |
| Ag | 77.56 | 34.27 |
| Totals | 100 | 100 |

**Figure 12.** EDX Spectra of silver nanoparticles

### 3.11 XRD analysis

The XRD of Silver Nanoparticles formed was measured within the 2θ range of 5° to 80°, as presented in Figure 13. The occurrence of sharp diffraction peaks indicates the crystalline character of the compound. The hkl values calculated imply a cubic crystal structure that is very similar to the standard JCPDS card No. 04-0783.

The size of AgNPs was found to be 7 ± 0.0015 nm by averaging the crystallite size. The diffractogram evidently shows three characteristic diffraction peaks at 38.1°, 44.3°, and 64.4°, which are assigned to the (111), (200), and (220) crystal planes, respectively. These peaks verify the face-centered cubic (FCC) crystal structure of bulk AgNPs [20].

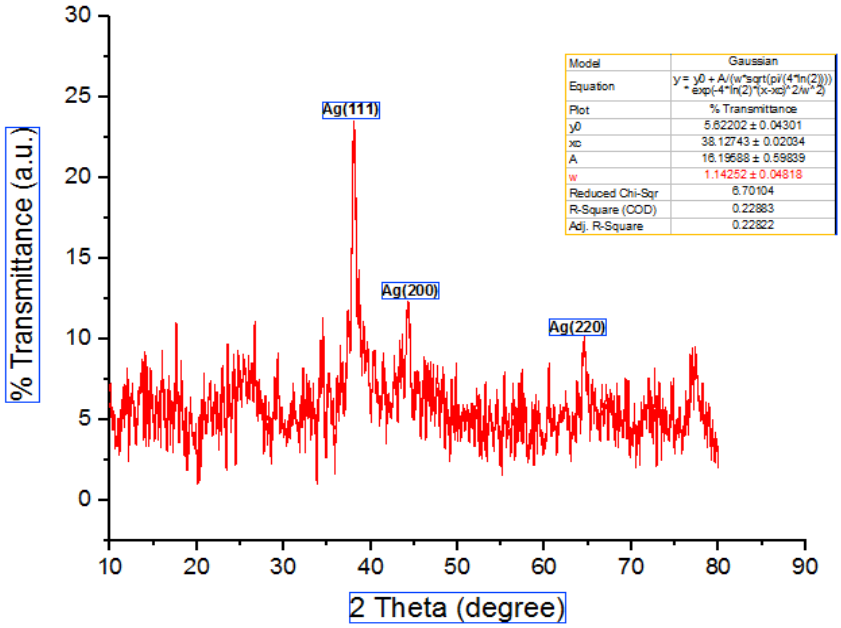


**Figure 13.** Diffractogram of AgNPs

### 3.12 Optimization of Lead (II) Concentration

A sensor system's sensitivity to the target analyte is an essential parameter. Figure 14 shows the impact of changing ion concentrations on the AgNP absorption intensity $Pb^{2+}$ concentrations were systematically adjusted between 0.01 and 10 µM concentrations while maintaining constant nanoparticle concentrations. With a correlation factor of $R^2 = 0.9936$ throughout a concentration range of 0.01–10 µM, a linear relationship between concentration and $Pb^{2+}$ absorption intensity was found. The linear equation slope and the standard deviation of the blank solution from the formula LOD = F × SD/b were used to compute the LOD of $Pb^{2+}$. Lead theoretical lower limit of detection was determined to be 4.02 nm, which is less than the previously stated.

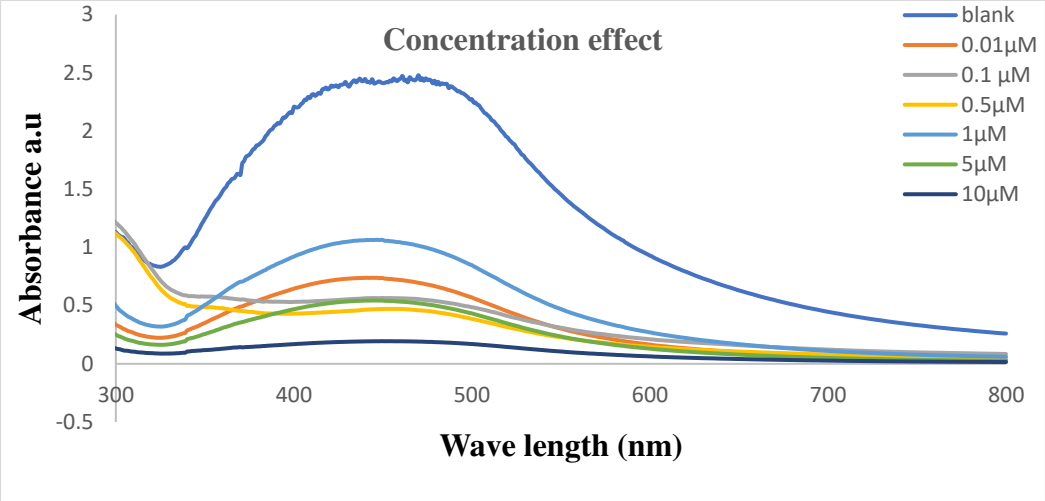


**Figure 14.** UV/Vis spectra of $Pb^{+2}$ sensing at different concentrations

### 3.13 Effect of pH on lead (II) sensing

The pH effect on $Pb^{2+}$ detection was explored using UV-Vis spectroscopy, as evident in Figure 15. Results indicate that pH significantly influences sensitivity and effectiveness of the sensing material. In basic conditions (pH 8, 9, 10), the material is more sensitive at low concentrations of $Pb^{2+}$ and indicates improved adsorption and interaction under alkaline conditions. Acidic conditions (pH 2, 3, 5) conversely create colorimetric sensing where detection is based on visible coloration instead of sharp absorbance peaks. This is indicative of a change in sensing mechanism at low pH levels that could be the result of surface modifications or alterations in solubility. Still, the original pH is preferred since extreme changes impact stability and performance. The results indicate the significance of pH control in achieving optimized $Pb^{2+}$ detection, with the conclusion that alkaline conditions are superior for high sensitivity in applications for lead ion sensing.

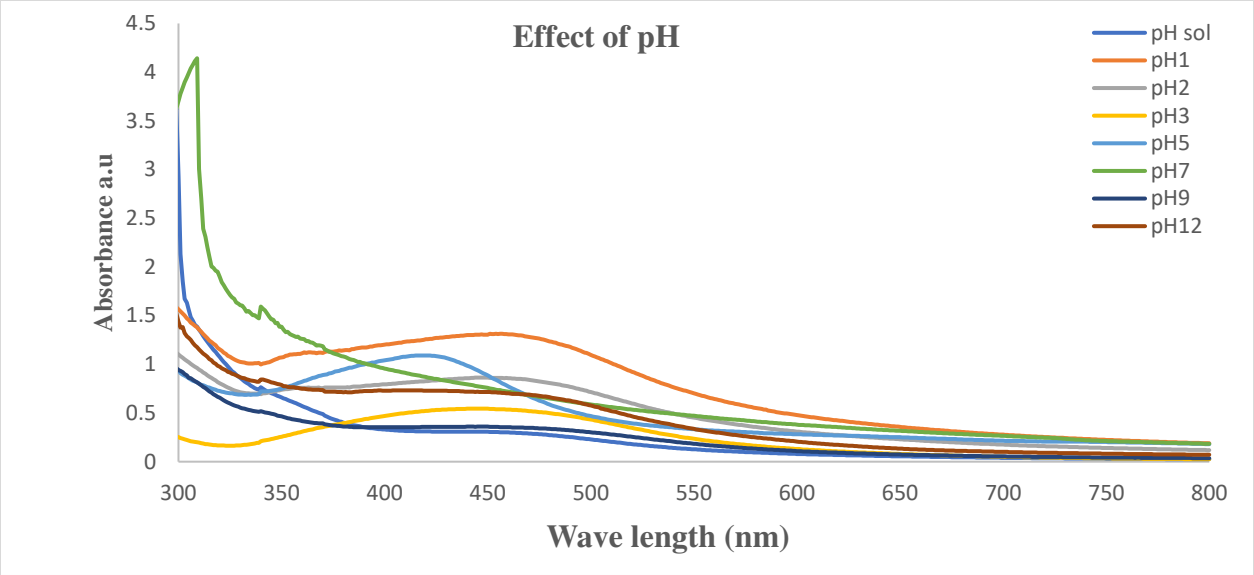


**Figure 15.** UV/Vis spectra of Lead(II) sensing at different pH

### 3.15 Reduction of 4-nitrophenol

The catalytic properties of synthesized silver nanoparticles were confirmed through testing their capability to reduce 4-NP using sodium borohydride. 4-Nitrophenol functions as a toxic substance due to its electron withdrawing nitro group which makes it difficult for basic degradation pathways to work effectively. The reduction process was spectrophotometrically monitored through the data presented in Figure 16. An absorption peak at 400 nm appeared in the UV spectra at t = 0 min indicating the production of nitrophenolate ions. The reaction of 4-aminophenol formation created a broad absorption band at 298 nm after the reduction of the initial absorption peak at 400 nm upon addition of biosynthesized AgNPs. The synthesized Ag NPs demonstrated efficient catalytic effectiveness through their solution color change from bright yellow to colorless within 8 minutes thus establishing the importance of this research. The reduction potential between 4-nitrophenol without AgNPs changed over time as monitored through absorbance measurement systems. It indicates that in the absence of AgNPs, 4-NP cannot be reduced using NaBH4 while with AgNPs they reduced 99.57% into 4-AP.

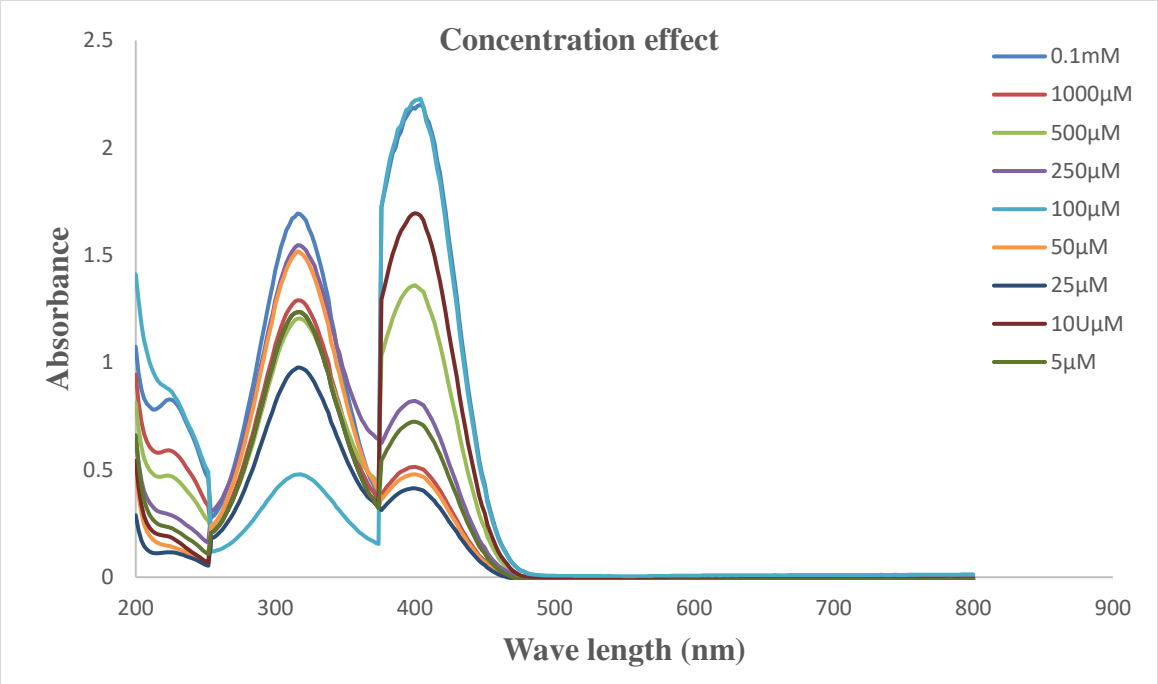


**Figure 16.** Optimization of 4-nitrophenol reduction at different concentration

### 3.16 Concentration optimization of reduction of 4-nitrophenol by AgNPs

The 4-NP regression and optimization analysis were examined using UV-Vis spectroscopy, as shown in Figures 17 and 18. Figure 17 shows absorbance trends for various 4-NP concentrations, from initial to final. Results show that high concentrations of 4-NP lead to high absorbance, which shows a visible concentration-optical response relationship. Initial absorbance values are higher than final values, which implies that the reaction or adsorption changes 4-NP's optical properties as time passes.

4-nitrophenol reduction was measured at a concentration of 0.1 µM, 5 µM, 25 µM, 50 µM, and 100 µM. AgNPs reduced 99.57%, 99.15%, 99.00%, 98.94%, 97.78%, 97.64%, and 93.67% of 4-nitrophenol, respectively. This is evidence of the effectiveness of AgNPs in 4-NP concentration reduction at various levels.

Figure.18 demonstrates high linear correlation ($R^2 = 0.9956$) of absorbance vs. concentration for 4-NP. The regression equation (y= 0.041x - 0.0241) indicates that absorbance is directly proportional to concentration, confirming UV-Vis spectroscopy's accuracy in quantifying 4-NP. These findings demonstrate the effectiveness of UV-Vis spectroscopy in detecting changes in 4-

NP concentration, and the efficiency of AgNPs in reduction gives credibility to its applicability in environmental remediation and analytical purposes.

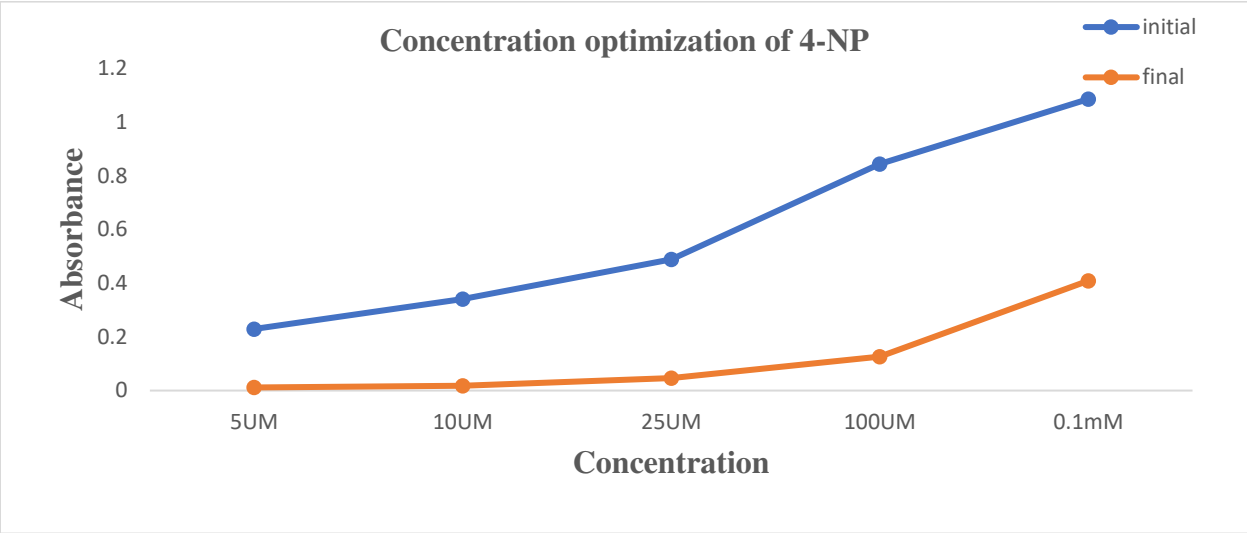


**Figure 17.** Concentration to absorbance graph of reduction of 4-nitrophenol with AgNPs

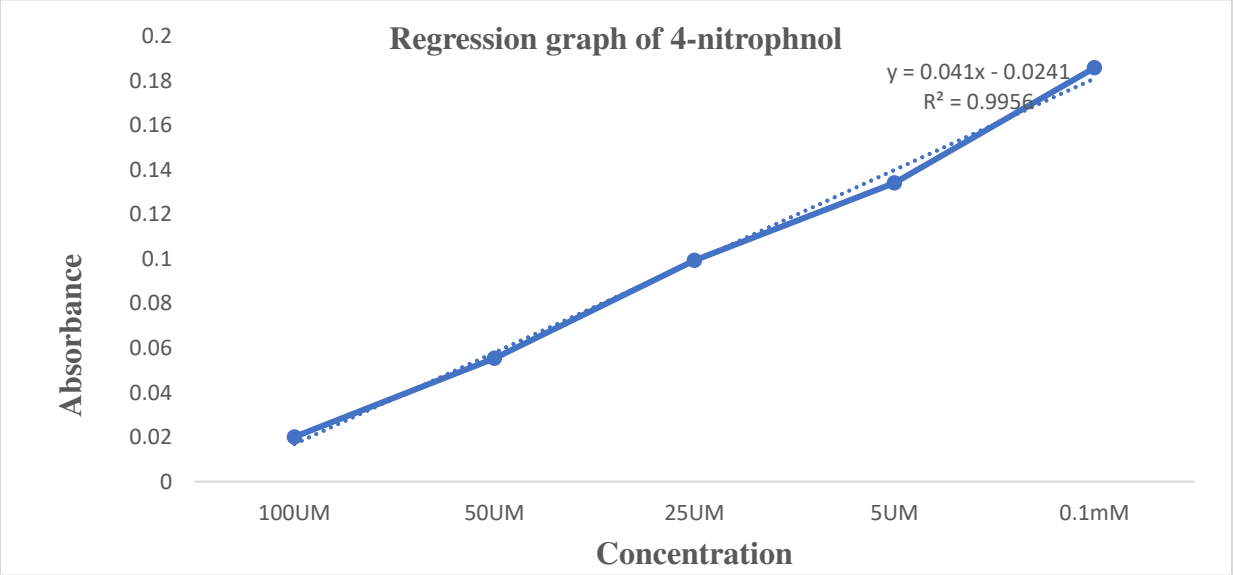


**Figure 18.** Regression graph of 4-nitrophenol

## 4. CONCLUSION

In this research, silver nanoparticles (AgNPs) were successfully prepared through a green synthesis process mediated by Cenchrus biflorus extract. The extract served as a reducing agent, as well as a stabilizing agent, in generating a cost-effective and eco-friendly production process. UV-Vis spectroscopy, FTIR, SEM, XRD, and EDX characterization verified the synthesis of AgNPs with favorable physicochemical features. Optimization of important reaction parameters, such as precursor concentration (0.1 mM $AgNO_3$), temperature (80°C), pH (7), reaction time (1 hour), and extract to $AgNO_3$ volumetric ratio (1:5), produced stable and highly active nanoparticles.

The synthesized silver nanoparticles (AgNPs) possessed effective catalytic activity in reducing 4-nitrophenol, with an efficiency of degradation close to 99.57% when utilized in the presence of sodium borohydride ($NaBH_4$). The AgNPs were also highly sensitive in the determination of lead ion ($Pb^{2+}$) across a broad range of concentrations (0.01 μM to 10 μM) and therefore is an excellent prospect for environmental analysis and water treatment.

The present study demonstrates the application potential of AgNPs mediated by Cenchrus biflorus as a green, multi-functional nanomaterial in environmental cleaning and heavy metal monitoring. Scale-up of the synthetic protocol and testing of long-term stability and recyclability of the nanoparticles in real-world contexts are proposed directions of future investigation.

**Acknowledgements**

The authors are grateful to the Department of Chemistry and the Department of Physics, Kohat University of Science and Technology (KUST), for the laboratory facilities and technical assistance needed during the research work process. There was no specific funding from any public, commercial, or not-for-profit funding organization for this study.

**Authors Contribution**

Muhammad Bilal started the process of detailing the planning of the research work, conducted the experiments with caution, and worked hard to gather and analyze the results of the

experiments. Majid Ali played a key role in supervising the research process, was in charge of writing the initial draft of the paper, and was in charge of all the communications with the journal to ensure that everything was in order. Rehana Yasmeen was also very supportive by giving guidance throughout the research, thoroughly reviewing and refining the paper, and playing the crucial role of corresponding author. Muhammad Qasim assisted with the lab work, conducted literature searches for the corresponding studies that were relevant to the research, and prepared the figures that presented the results. Lastly, all authors took the effort to read through and approved the final version of the paper prior to submission.

## Conflicts of Interest or Competing Interests

The authors declare that they have no conflicts of interest or competing interests.

## Data and Code Availability

The data underpinning the findings of this research are accessible from the lead authors on reasonable request. There was no code used or developed in this research.

## Supplementary Information

N/A

## Ethical Approval

N/A

## REFERENCES


[1] Abuelma'atti M (2009) Nanotechnology: Benefits, risks and ethical issues. In: 2009 5th IEEE GCC Conference & Exhibition. IEEE, pp. 1–5.

[2] Roco M (2003) Broader societal issues of nanotechnology. Journal of Nanoparticle Research 5:181–189.

[3] Cygan G (2001) Molecular modeling in mineralogy and geochemistry. Molecular Modeling Theory: Applications in the Geosciences 42:1–35.

[4] Moodley J, Krishna S, Pillay K, Govender S (2018) Green synthesis of silver nanoparticles from Moringa oleifera leaf extracts and its antimicrobial potential. Advances in Natural Sciences: Nanoscience and Nanotechnology 9:015011–015021.

[5] Thompson D, Stokes R, Martin R, Lundahl P, Faulds K, Graham D (2008) Synthesis of unique nanostructures with novel optical properties using oligonucleotide mixed-metal nanoparticle conjugates. Small 4:1054–1057.

[6] Manmode A, Sakarkar D, Mahajan N (2009) Nanoparticles—tremendous therapeutic potential: a review. International Journal of PharmTech Research 1:1020–1027.

[7] Gu F, Wang S, Lü M, Zhou G, Xu D, Yuan C (2004) Photoluminescence properties of $SnO_2$ nanoparticles synthesized by sol–gel method. The Journal of Physical Chemistry B 108:8119–8123.

[8] Lu A, Salabas E, Schüth F (2007) Magnetic nanoparticles: synthesis, protection, functionalization, and application. Angewandte Chemie International Edition 46:1222–1244.

[9] Shanmuganathan R, et al. (2019) Synthesis of silver nanoparticles and their biomedical applications—a comprehensive review. Current Pharmaceutical Design 25:2650–2660.

[10] Adhikari A, Lamichhane L, Adhikari A, Gyawali G, Acharya D, Baral E, et al. (2022) Green synthesis of silver nanoparticles using Artemisia vulgaris extract and its application toward catalytic and metal-sensing activity. Inorganics 10:113–131.

[11] Doan V, Phan T, Vasseghian Y, Evgenievna L (2022) Efficient and fast degradation of 4-nitrophenol and detection of Fe(III) ions by Poria cocos extract stabilized silver nanoparticles. Chemosphere 286:131894–131903.

[12] Lee S, Begildayeva T, Yeon S, Naik S, Ryu H, Kim T (2021) Eco-friendly synthesis of lignin-mediated silver nanoparticles as a selective sensor and their catalytic removal of aromatic toxic nitro compounds. Environmental Pollution 269:116174–116187.

[13] Ahmed F, Kabir H, Xiong H (2020) Dual colorimetric sensor for $Hg^{2+}$/$Pb^{2+}$ and an efficient catalyst based on silver nanoparticles mediating by the root extract of Bistorta amplexicaulis. Frontiers in Chemistry 8:591958–591971.

[14] Choudhury R, Misra T (2018) Gluconate stabilized silver nanoparticles as a colorimetric sensor for $Pb^{2+}$. Colloids and Surfaces A: Physicochemical and Engineering Aspects 545:179–187.

[15] Qi L, Shang Y, Wu F (2012) Colorimetric detection of lead(II) based on silver nanoparticles capped with iminodiacetic acid. Microchimica Acta 178:221–227.

[16] Iravani S, Korbekandi H, Mirmohammadi S, Zolfaghari B (2014) Synthesis of silver nanoparticles: chemical, physical and biological methods. Research in Pharmaceutical Sciences 9(6):385–397.

[17] Movasaghi Z, Rehman S, ur Rehman D I (2008) Fourier transform infrared (FTIR) spectroscopy of biological tissues. Applied Spectroscopy Reviews 43(2):134–179.

[18] Kashin A, Ananikov V (2011) A SEM study of nanosized metal films and metal nanoparticles obtained by magnetron sputtering. Russian Chemical Bulletin 60(12):2602–2607.

[19] Skorikov A, Heyvaert W, Albecht W, Pelt D, Bals S (2021) Deep learning-based denoising for improved dose efficiency in EDX tomography of nanoparticles. Nanoscale 13(28):12242–12249.

[20 ]Deepty M (2019) XRD, EDX, FTIR and ESR spectroscopic studies of co-precipitated Mn-substituted Zn-ferrite nanoparticles. Ceramics International 45(6):8037–8044.